

Quantitative evaluation of ischemic myocardial scar tissue by unenhanced T1 mapping using 3.0 Tesla MR scanner

Aylin Okur, Mecit Kantarcı, Yeşim Kızrak, Sema Yıldız, Berhan Pirimoğlu, Leyla Karaca, Hayri Oğul, Serdar Sevimli

PURPOSE

We aimed to use a noninvasive method for quantifying T1 values of chronic myocardial infarction scar by cardiac magnetic resonance imaging (MRI), and determine its diagnostic performance.

MATERIALS AND METHODS

We performed cardiac MRI on 29 consecutive patients with known coronary artery disease (CAD) on 3.0 Tesla MRI scanner. An unenhanced T1 mapping technique was used to calculate T1 relaxation time of myocardial scar tissue, and its diagnostic performance was evaluated. Chronic scar tissue was identified by delayed contrast-enhancement (DE) MRI and T2-weighted images. Sensitivity, specificity, and accuracy values were calculated for T1 mapping using DE images as the gold standard.

RESULTS

Four hundred and forty-two segments were analyzed in 26 patients. While myocardial chronic scar was demonstrated in 45 segments on DE images, T1 mapping MRI showed a chronic scar area in 54 segments. T1 relaxation time was higher in chronic scar tissue, compared with remote areas (1314 ± 98 ms vs. 1099 ± 90 ms, $P < 0.001$). Therefore, increased T1 values were shown in areas of myocardium colocalized with areas of DE and normal signal on T2-weighted images. There was a significant correlation between T1 mapping and DE images in evaluation of myocardial wall injury extent ($P < 0.05$). We calculated sensitivity, specificity, and accuracy as 95.5%, 97%, and 96%, respectively.

CONCLUSION

The results of the present study reveal that T1 mapping MRI combined with T2-weighted images might be a feasible imaging modality for detecting chronic myocardial infarction scar tissue.

In ischemic cardiac diseases, differentiating viable from nonviable myocardial tissue is important for clinical decision-making (1). The viable myocardium with decreased blood-flow such as hibernating or stunned myocardium will recover function following coronary revascularization, whereas during the chronic stage of infarction, a dense fibrotic scar replaces the infarcted myocardium and this scar tissue will not recover function (2). Sometimes more aggressive treatment is needed to improve blood flow such as angioplasty, stenting, and coronary artery bypass surgery. Therefore, evaluation of viability is critical for myocardium.

Positron-emission-tomography, single-photon-emission computed tomography and dobutamine echocardiography are noninvasive techniques for assessing myocardial viability. Although these techniques have proven use in clinical practice, there are several limitations that may reduce their diagnostic accuracy (3). Infarcted or noninfarcted myocardium is determined arbitrarily within a viewing window (i.e., the range of gray/color values to be selected for viewing) by these techniques (4). Therefore, assessment of myocardial viability will vary qualitatively and subjectively due to the pitfalls of the techniques.

Recently, delayed contrast-enhancement (DE) cardiac magnetic resonance imaging (MRI) has been used for an increasing number of clinical applications in cardiac diseases. However, there are conflicting reports concerning the utility of contrast-enhanced MRI after infarct healing. Firstly, this method makes a qualitative assessment of myocardial fibrosis, similar to previously mentioned methods. In addition, with conventional DE-MRI sequences, signal intensity is expressed on an arbitrarily scale that differs from one imaging to another. Therefore, this method is not suitable for direct signal quantification (5). Furthermore, concerns about the increased risk of gadolinium-induced nephrogenic systemic fibrosis have increased gradually in populations with impaired renal function (6, 7).

T1 mapping is a novel cardiac MRI technique and it allows measurements of absolute T1 relaxation times for each pixel (8). This technique involves the sampling of signal recovery during multiple measurements following a preparation pulse. The resulting relaxation time is then determined for each pixel contained in a parametric image, referred to as T1 mapping (9). In contrast to other imaging techniques, T1 mapping achieves signal quantification (in milliseconds) on a standardized scale. It reflects tissue changes without need for signal intensity thresholds, post-processing, reference region-of-interest, or contrast material. The quantitative evaluation of myocardial T1 values (T1 mapping) has been

From the Department of Radiology (A.O. ✉ draylinokur@hotmail.com), Bozok University, School of Medicine, Yozgat, Turkey; the Departments of Radiology (A.O., M.K., Y.K., B.P., L.K., H.O.) and Cardiology (S.S.), Atatürk University, School of Medicine, Erzurum, Turkey; the Department of Radiology (S.Y.), Harran University School of Medicine, Şanlıurfa, Turkey.

Received 2 January 2014; revision requested 6 February 2014; revision received 17 February 2014; accepted 2 March 2014.

Published online 18 June 2014.
DOI 10.5152/dir.2014.13520

used recently to identify patients with diffuse fibrosis or myocarditis, or acute and chronic myocardial infarction (MI) (4, 10). In addition, although previous studies show that MI quantification can be achieved using a magnetic field strength of 1.5 Tesla (T) (7), to our knowledge, these values have not yet been reported on chronic infarction for 3.0 T cardiac MRI.

The purpose of this study was to use high-resolution unenhanced T1 mapping to investigate the feasibility of using 3.0 T cardiac MRI to detect scar areas in myocardium resulting from chronic MI.

Materials and methods

This prospective study was approved by the institutional ethics committee, and written informed consent was obtained from all patients before enrollment.

Between June 2012 and October 2013, twenty-nine consecutive patients with known coronary artery disease (CAD) underwent cardiac MRI scanning at least six months after the onset of symptoms at the Atatürk University Medical School for assessment of myocardial scar tissue. Inclusion criteria were previous MI established on the basis of serum cardiac markers, positive nuclear stress testing results and/or proven CAD in coronary catheter angiography or computed tomography angiography (at least one coronary artery stenosis of $\geq 70\%$).

Exclusion criteria were findings of acute MI (clinical and laboratory), known cardiomyopathy, severe heart valve disease, systemic inflammatory conditions requiring any anti-inflammatory drugs, contraindications to cardiac MRI such as implanted pacemakers, defibrillators, or other metallic implants, and claustrophobia. Before cardiac MRI was performed, acute MI was excluded in all patients according to standard criteria by the referring physicians. Therefore, these patients represented a population with a high prevalence of chronic ischemic changes in the myocardium. Delayed-phase contrast-enhanced MRI was used as the noninvasive gold standard to evaluate the accuracy of T1 mapping technique for the assessment of myocardial scar tissue.

Magnetic resonance imaging

All patients were examined with a 3.0 T MRI (Magnetom Skyra, Siemens Healthcare, Berlin, Germany) using a 16-channel cardiac coil placed around the patient's chest. Patients were imaged in the supine position; image acquisition was performed during a single breath-hold to eliminate respiratory motion artefacts. Following routine cardiac MRI examination, T2-weighted, T1 mapping, and DE imaging sequences were performed with matching short-axis images. Twelve slices were obtained per each image acquisition. T1 mapping was performed using the modified Look-Locker inversion recovery (MOLLI) (11), followed by black-blood T2-weighted imaging. All images were acquired before administration of contrast agents. DE-MR imaging was obtained using a T1-weighted phase-sensitive sequence 8–10 minutes after intravenous administration of a contrast agent (0.1 mmol/kg at 6 mL/s gadopentetate dimeglumine (Gd-DTPA, Magnevist, Bayer Healthcare, Berlin, Germany).

For T2-weighted images, the electrocardiographic (ECG)-gated, black-blood, half-Fourier acquisition single-shot turbo spin-echo (HASTE) sequences were performed with the following image parameters: TR, $2 \times RR$; TE, 65 ms; TI, 140 ms, in basal, mid-ventricular, and apical short-axis slices (slice thickness, 8 mm; gap, 5 mm; field of view, 34×38 cm; matrix, 256×256 ; NEX, 1).

A MOLLI pulse sequence was performed, as described previously. Twelve source images taken during one breath-hold (16–20 s) are obtained in this procedure. This permits one parametric T1 mapping to be reconstructed. Source images were all identical to one another (same voxel size, image position and cardiac cycle phase), apart from different effective TIs. In order to achieve this, we performed three separate ECG-triggered inversion recovery-prepared experiments (TI 100, 200, and 350 ms). Several single-shot images (200 ms) were subsequently acquired at end-diastole of consecutive heartbeats. The readout involved a balanced steady-state free precession (bSSFP) sequence (TR, 3.9 ms; TE, 1.95 ms; flip angle, 50° ; sensitivity-encoding

(SENSE) factor, 2; field of view, 380×342 mm; matrix, 240×151 ; slice thickness, 8 mm). Once the SENSE reference scan had been obtained, unenhanced MOLLI sequences were obtained at the mid-cavity, basal, and apical short-axis levels. These were defined as the central three of five short-axis slices located between the mitral annulus and the left ventricular tip at systolic long-axis cine images (12).

Phase-sensitive inversion recovery sequence: voxel size, $2.0 \times 1.5 \times 8.0$ mm; matrix, 144×256 ; TR/TE, 800.20/3.36 ms; flip angle, 25° .

MRI examination lasted approximately 3 min for T2-weighted images, 5 min for T1 mapping, and 10 min for DE images. The images obtained were stored in DICOM format.

Image evaluation

All images were transferred to a workstation (Syngo Via Console, software version 2.0, Siemens AG Medical Solutions, Erlangen, Germany) for evaluation. All MR image series were analyzed in separate readout sessions with one week intervals (first session, T1 mapping images; second session, DE images) in random order by three radiologists in consensus. The observers were experienced in the field of cardiovascular imaging (M.K., ten years of experience; A.O. and Y.K., three years of experience).

Matched short-axis slices were compared across T2-weighted imaging, T1 mapping, and DE imaging. Myocardial signal changes were evaluated on T2-weighted images. Parametric T1 relaxation time pixel maps were automatically generated from the MOLLI sequence images, without the need for further post-processing, accelerating the whole process. The program produced a nonlinear three-parameter curve fit on the source data sets. It also automatically determined the T1 time for each pixel and produced parametric T1 mapping. The epicardial and endocardial contours of left ventricular myocardium was later defined automatically with commercially available software on a workstation. A region-of-interest of approximately 3 cm^2 was placed in the remote myocardium (nonbright area) and the infarct tissue (bright area) on T1 mapping

images, therefore mean T1 relaxation times of these areas were measured (Fig. 1).

The myocardium was divided into 17 equiangular segments using the American Heart Association's segmentation of the left ventricular myocardium (13). Infarction area dimensions inside each segment were estimated visually. Categorization was then performed on the basis of the percentage enhanced area of each segment (damaged area/segmental area) on T1 mapping and DE images: 0, normal; 1, 1%–25%; 2, 26%–50%; 3, 51%–75%; 4, >75% (3).

Compared with normal myocardium, DE was defined as an increased signal intensity area. DE images were judged to be of ischemic origin in patients with a history of known chronic MI and/or proven CAD. T1 relaxation values and diagnostic performance of T1 mapping in chronic MI were evaluated. Sensitivity and specificity values were calculated for T1 mapping with DE images considered as the gold standard.

In addition, routine cardiac assessments were performed, such as quantification of left ventricular volumes, ejection fraction, and wall motion abnormalities using Syngo Via Console software by cine images.

Statistical analysis

Normality of data was tested using the Kolmogorov-Smirnov test. Normally distributed data is presented as mean±standard deviation; nonparametric data is presented as medians with interquartile ranges. The association of T1 relaxation times in myocardial scar and normal myocardial tissue was evaluated by Spearman rank correlation and Pearson correlation tests. All interpretations were two sided, and $P < 0.05$ was assumed as statistically significant. The sensitivity, specificity, and accuracy rates were calculated for T1 mapping on the myocardial scar tissues compared with DE images that was postulated as gold standard.

Results

Characteristics of patients are presented in Table 1. Of the 29 patients enrolled, three patients were excluded due to inability to hold breath (n=1) and poor image quality (n=2). The fi-

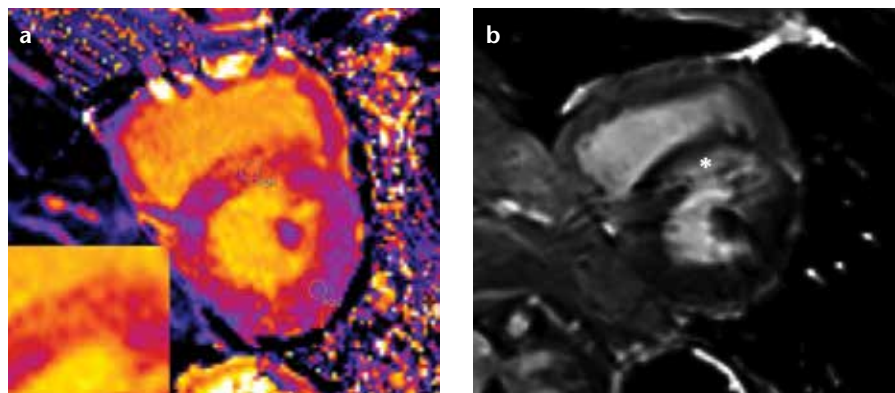


Figure 1. a, b. A 70-year-old man with a known history of myocardial infarction. T1 mapping short-axis image (a) shows transmurular infarction areas of segments 7 and 8 (ROI-1) as bright (T1 relaxation time, 1368±61 ms). The magnified image of septal scar tissue is demonstrated as an inset on the left corner. The same image shows relaxation time of remote myocardium (ROI-2, T1 relaxation time: 1129±75 ms). DE-MRI (b) image shows transmurular extent of delayed enhancement within the same segments (*asterisk*).

Table 1. Characteristics of the patients (n=26)

Parameter	
Age (years), mean±SD	64.4±10.4
Sex, n	
Male	23
Female	3
Risk factors, n (%)	
Smoking	12 (46)
Hypertension	11 (42)
Diabetes	4 (15)
Family history	15 (57)
Culprit coronary artery, n (%)	
LAD	15 (57)
LCx	3 (11)
RCA	10 (38)
Ejection fraction (%), mean±SD	39.5±7.1

SD, standard deviation; LAD, left anterior coronary artery; LCx, left circumflex; RCA, right coronary artery.

nal study cohort consisted of 26 patients (23 men, 3 women; mean age, 64±10.4 years). Four hundred and forty-two segments of 26 patients were analyzed. All patients underwent the complete examination without complications.

None of the patients had abnormal signal intensity indicative of active edema on T2-weighted phase sensitive inversion recovery images. In T1 mapping images, myocardial chronic scar was demonstrated in 54 segments. Nine segments, visualized as normal on DE images, were reported as scar tissue

on T1 mapping (false positive). The wall involvement of the false positive segments was one segment in group 1 (1%–25%), four segments in group 2 (25%–50%), and two segments in group 3 (50%–75%). Two segments in group 4 (>75%) were localized at the level of the aortic outflow tract. In DE images, myocardial chronic scar was demonstrated in 45 segments. None of these segments displayed an isolated nonischemic (subepicardial) pattern on DE images. Distribution of affected segments was shown in Table 2 for T1 mapping and DE-MRI. Comparison of

Table 2. Distribution of myocardial infarction based on segments for T1 map and DE-MRI

Segments	DE-MRI	T1 map
Basal segments		
1	-	-
2	-	-
3	4	6
4	4	7
5	2	2
6	-	-
Midventricular segments		
7	4	5
8	4	4
9	6	6
10	9	11
11	8	7
12	2	3
Apical segments		
13	-	-
14	2	3
15	-	-
16	-	-
17	-	-
Total	45	54

DE-MRI, delayed contrast-enhancement magnetic resonance imaging.

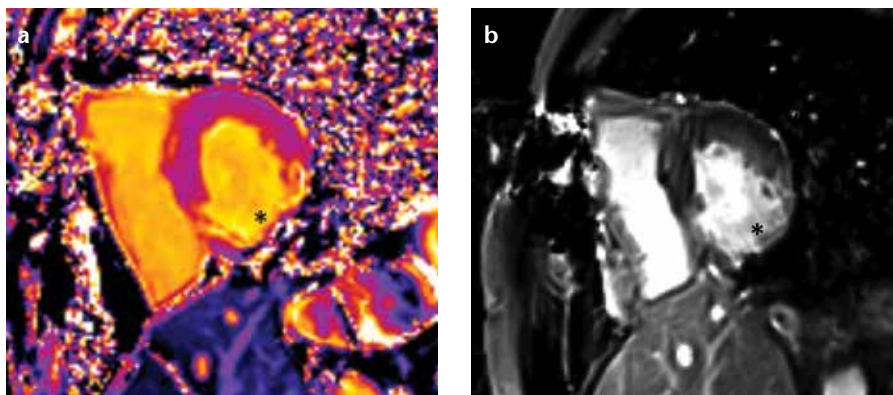


Figure 2. a, b. A 68-year-old man with a known history of myocardial infarction. T1 mapping image (a) shows transmurally infarcted areas of segments 9, 10, and 11 (asterisk) as bright. Delayed contrast-enhancement MRI (b) demonstrates transmurally infarcted areas within the same segments (asterisk).

extent of injury within myocardium for both techniques is shown in Table 3. There was a significant difference between T1 mapping and DE images in the evaluation of myocardial wall injury extent ($P < 0.05$).

In order to investigate the accuracy of T1 values in comparison with DE

images, we first evaluated the variability of T1 values in unaffected myocardial segments (as confirmed by DE and T2-weighted images). Later, we assessed the T1 relaxation times in scar areas (as verified by DE and T2-weighted images). In chronic scar tissue, the T1 relaxation time of bright areas was

higher than the remote myocardial tissue (1314 ± 98 ms vs. 1099 ± 90 ms, $P < 0.001$, Fig. 2). The correlation between scar tissue and normal myocardial tissue for T1 mapping is shown in Fig. 3. Therefore, increased T1 values were shown in areas of myocardium colocalized with areas of DE and normal signal on T2-weighted images.

Segmental visual wall motion abnormalities were seen in 38 of 45 abnormal segments. The mean left ventricular ejection fraction was $39.5\% \pm 7.1\%$ (range, 30%–55%). A significant difference was found between hypokinetic and normokinetic segments for T1 values ($P = 0.001$). T1 values increased significantly in hypokinetic segments. Mean T1 map relaxation times were 1359 ± 41 ms in normokinetic segments, and 1128 ± 34 ms in hypokinetic segments.

T1 mapping and DE imaging demonstrated excellent performance for the assessment of myocardial scar areas. We calculated sensitivity, specificity, and accuracy of T1 mapping as specificity, 95.5%, 97.7% accuracy 97.5%, respectively (Table 4).

Discussion

Our results suggest that unenhanced T1 mapping in combination with T2-weighted MRI might be used for evaluating chronic MI (no hyperintensity on T2-weighted images and increased T1 relaxation time in bright areas compared with the normal myocardium) and normal myocardium (no hyperintensity, lower T1 relaxation time, and no bright area compared with the abnormal myocardium). Therefore, unenhanced T1 mapping may serve as a complementary technique to T2-weighted imaging for assessing chronic myocardial scars in ischemic heart diseases.

Clinical decisions (i.e., medical vs. interventional therapy) frequently rely on being able to differentiate reversible from irreversible or acute from chronic myocardial injury and knowing the extent of myocardial injury (14), so that unnecessary invasive procedures may be prevented. Currently, myocardial injury characterization by MRI is most commonly performed using T2-weighted and contrast-enhanced imaging (15), where substantial differences be-

Table 3. Distribution of segments according to wall involvement groups

Wall involvement	DE-MRI	T1 map
Group 0	397	388
Group 1	0	1
Group 2	25	28
Group 3	8	11
Group 4	12	14
Total segments	442	442

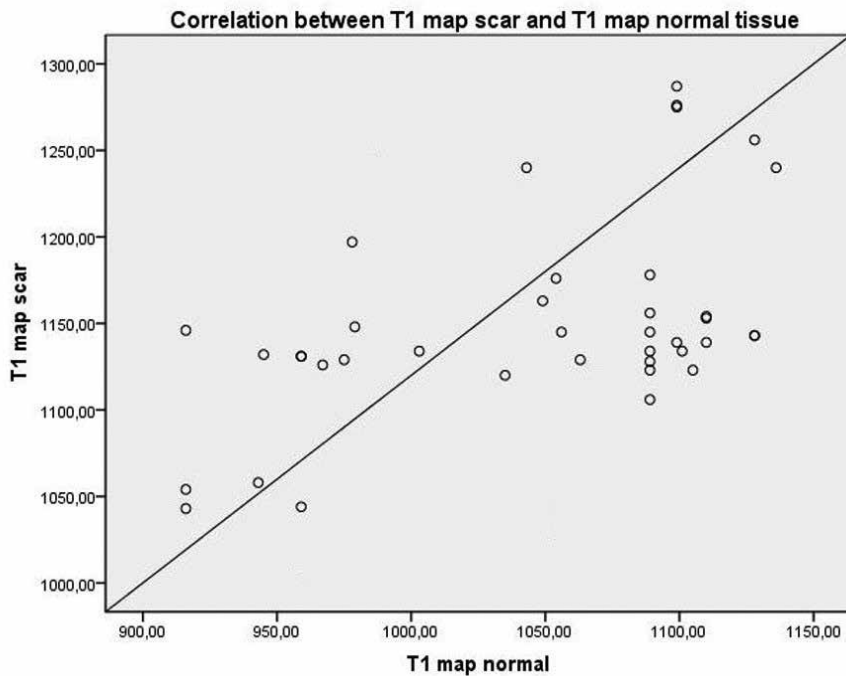
Wall involvement: group 0, normal; group 1, 1%–25% involved; group 2, 25%–50% involved; group 3, 51%–75% involved; group 4, >75% involved.
DE-MRI, delayed contrast-enhancement magnetic resonance imaging.

Table 4. A comparison between the routine DE-MRI and T1 mapping findings (n=442)

T1 map MRI				DE-MRI		Sensitivity* (%)	Specificity* (%)	Accuracy* (%)
TP	TN	FP	FN	TP	TN			
43	388	9	2	45	397	95.5	97.7	97.5

*Sensitivity, specificity, and accuracy of the T1 map images.

DE, delayed enhancement; FN, false negative; FP, false positive; TN, true negative, TP, true positive.

**Figure 3.** Graph shows correlation between scar tissue and normal myocardial tissue for T1 mapping.

tween acute and chronic myocardial injuries may sometimes be missed (3). Both acute and chronic MI display DE, regardless of their age (15–17). Some studies have shown fully functional improvement and regression of DE within the ischemic myocardium in follow-ups (18–20). Therefore, DE images have challenged the view that acute DE

equals stable irreversible myocardial injury and the clinical importance of DE has recently been become questionable. It also requires extended imaging times and is restricted in its accuracy for precise quantification of myocardial scar tissue.

T2-weighted MRI is the standard imaging technique for detecting acute

myocardial edema, although myocardial edema is not an expected finding in myocardial chronic scar tissue (21). We also did not determine high signal intensity in scar area on T2-weighted images.

Cardiac T1 mapping MRI is a technique that enables myocardial signal quantification on a standard scale (10, 22–24). This novel technique involves the sampling of signal recovery during multiple measurements following a preparation pulse. The resulting relaxation time is then determined for each pixel contained in a parametric image, known as T1 mapping (9). The most widely used T1 mapping sequence is based on the MOLLI technique and has been described by Messroghli et al. (10, 23, 24). We also used the MOLLI technique in our study. Advantages of the MOLLI sequence include T1 relaxation time at the same phase of the cardiac cycle, thus permitting more reliable T1 measurements, less dependence on heart rate, and the use of a single breath-hold (23). T1 mapping makes it possible to bypass windowing and signal enhancement variations by calculating T1 relaxation times directly, compared to DE images. This in turn permits signal quantification (in milliseconds) of each myocardial voxel and subsequent standardized characterization of myocardial tissue (5).

Each tissue exhibits a specific range of T1 values, although these values are not tissue-specific (25). Previous studies on myocardial fibrosis suggested unenhanced mean T1 values of 977 ± 63 ms in normal myocardium compared with 1060 ± 61 ms in myocardial fibrosis areas at 1.5 T (26). Our data also revealed marked changes in T1 relaxation time within the infarct zone compared with normal myocardium. We found T1 values around 1099 ± 90 ms in normal myocardium (nonbright area) compared to 1314 ± 98 ms in chronic infarction tissue (bright area) for T1 mapping at 3.0 T MRI. Unenhanced T1 values of myocardial fibrosis (infarct scar) were shown significantly higher than those of normal myocardium in the present study. The changes in myocardial T1 values measured on MRI appear to reflect an increase in collagen (fibrosis) in the myocardium secondary to chronic MI, compared with normal myocardium.

We failed to demonstrate scar tissue in only two segments. When these seg-

ments were analyzed, we determined that the extent of DE was 25%–50% and located in the left ventricular free wall. In addition, nine segments were reported as normal in DE images, while these segments were evaluated as chronic scar tissue in T1 mapping. When we evaluated retrospectively, we discovered that two of these segments were located at the level of the aortic outflow tract. As known, partial volume effects typically lead to troubles near the aortic outflow tract (27). Infarction size was small in one segment. It may be difficult to distinguish bright blood between the myocardium and papillary muscles and myocardial scar in T1 mapping. Differentiating minor subendocardial MIs from the blood pool may also be problematic, since both have a bright appearance. This information may be an explanation for the remaining segments. By evaluating images according to a particular coronary territory, we can avoid these pitfalls. Ischemic areas are known to be localized in the subendocardial area and definitely conform to one of the particular coronary territories.

Previous studies reported that the extent of nonviable tissue in a myocardial segment can be used to predict recovery of function after revascularization (28). It is generally unlikely that myocardial scar or fibrosis in which more than 50% of myocardial wall thickness is involved at cardiac MR imaging will resume contractile function in the wake of coronary revascularization (2). DE-MRI is now considered the reference standard for direct visualization of nonviable myocardial tissue. Our results also indicate that T1 mapping allows for the assessment of the extent of segmental scar area. Diagnostic value of T1 mapping MRI was found to be comparable to DE images for the myocardial scar extent. In addition, our study demonstrated that T1 relaxation time increased significantly in regional wall motion abnormalities. T1 mapping values were also found higher in hypokinetic areas.

One advantage of combined application of T1 mapping and T2-weighted images, compared with combined application of T2-weighted and DE-MRI, is the reduction in acquisition time (8 min vs. 13 min). Moreover,

the diagnostic values of these combinations are very close to each other. We reported that T1 mapping detected chronic scar tissue caused by chronic MI with 95.5% sensitivity and 97.7% specificity.

Several limitations of the present study should be considered. Firstly, this study was a cross-sectional study with a small sample size. Secondly, we did not provide histopathological confirmation of our findings; coronary artery distribution, previous infarction history and no findings of acute MI were considered as evidence of chronic infarction. Finally, we have not investigated the impact of the T1 mapping technique on the clinical outcome, as this was not an objective of this study.

In conclusion, this study highlights certain key points for the evaluation of myocardial scar tissue. First, T1 mapping using standardized imaging protocols combined with T2-weighted images may be of great help for more accurate myocardial tissue characterization. T1 mapping can be used to distinguish between myocardial scars and normal myocardium, while T2-weighted imaging indicates the area of the acute or chronic event. Second, in selected cases, such as patients with impaired renal function, the gadolinium induced nephrogenic systemic fibrosis may be avoided using a combination of T1 mapping and T2-weighted MRI.

Conflict of interest disclosure

The authors declared no conflicts of interest.

References

1. Gersh BJ, Anderson JL. Thrombolysis and myocardial salvage: results of clinical trials and the animal paradigm. *Circulation* 1993; 88:296–306. [\[CrossRef\]](#)
2. Vogel-Claussen J, Rochitte CE, Wu KC, et al. Delayed enhancement MR imaging: utility in myocardial assessment. *Radiographics* 2006; 26:795–810. [\[CrossRef\]](#)
3. Kim RJ, Wu E, Rafael A, Chen EL, et al. The use of contrast-enhanced magnetic resonance imaging to identify reversible myocardial dysfunction. *N Engl J Med* 2000; 343:1445–1453. [\[CrossRef\]](#)
4. Messroghli DR, Walters K, Plein S, et al. Myocardial T1 mapping: application to patients with acute and chronic myocardial infarction. *Magn Reson Med* 2007; 58:34–40. [\[CrossRef\]](#)

5. Belloni E, Marchesi G, Aschieri D, et al. Inversion time prolongation at late enhancement cardiac MRI in a myeloma patient. *Diagn Interv Radiol* 2012; 18:552–554.
6. Ozbek O, Acar K, Kayrak M, et al. Relationship between color M-mode echocardiography flow propagation and cardiac iron load on MRI in patients with thalassemia major. *Diagn Interv Radiol* 2012; 18:208–214.
7. Mewton N, Liu CY, Croisille P, Bluemke D, Lima JA. Assessment of myocardial fibrosis with cardiovascular magnetic resonance. *J Am Coll Cardiol* 2011; 57:891–903.
8. Lim RP, Hecht EM, Xu J, et al. 3D non-gadolinium-enhanced ECG-gated MRA of the distal lower extremities: preliminary clinical experience. *J Magn Reson Imaging* 2008; 28:181–189. [\[CrossRef\]](#)
9. Edelman RR, Sheehan JJ, Dunkle E, Schindler N, Carr J, Koktzoglou I. Quiescent-interval single-shot unenhanced magnetic resonance angiography of peripheral vascular disease: technical considerations and clinical feasibility. *Magn Reson Med* 2010; 63:951–958. [\[CrossRef\]](#)
10. Dall'Armellina E, Ferreira VM, Kharbanda RK, et al. Diagnostic value of pre-contrast T1 mapping in acute and chronic myocardial infarction. *JACC Cardiovasc Imaging* 2013; 6:739–742. [\[CrossRef\]](#)
11. Kaldoudi E, Williams CR. Relaxation time measurements in NMR imaging. I. Longitudinal relaxation time. *Concepts Magn Reson* 1993; 5:217–242. [\[CrossRef\]](#)
12. Messroghli DR, Niendorf T, Schulz-Menger J, Dietz R, Friedrich MG. T1 mapping in patients with acute myocardial infarction. *J Cardiovasc Magn Reson* 2003; 5:353–359. [\[CrossRef\]](#)
13. Lee JJ, Liu S, Nacif MS, et al. Myocardial T1 and extracellular volume fraction mapping at 3 Tesla. *J Cardiovasc Magn Reson* 2011; 13:75. [\[CrossRef\]](#)
14. Rajappan K, Bellenger NG, Anderson L, Pennell DJ. The role of cardiovascular magnetic resonance in heart failure. *Eur J Heart Fail* 2000; 2:241–252. [\[CrossRef\]](#)
15. Lima JAC, Judd RM, Bazille A, Schulman SP, Atalar E, Zerhouni EA. Regional heterogeneity of human myocardial infarcts demonstrated by contrast-enhanced MRI: potential mechanisms. *Circulation* 1995; 92:1117–1125. [\[CrossRef\]](#)
16. Abdel-Aty H, Zagrosek A, Schulz-Menger J, et al. Delayed enhancement and T2-weighted cardiovascular magnetic resonance imaging differentiate acute from chronic myocardial infarction. *Circulation* 2004; 109:2411–2416.
17. Choi KM, Kim RJ, Gubernikoff G, Vargas JD, Parker M, Judd RM. Transmural extent of acute myocardial infarction predicts long-term improvement in contractile function. *Circulation* 2001; 104:1101–1107. [\[CrossRef\]](#)

18. Wu E, Judd RM, Vargas JD, et al. Visualisation of presence, location, and transmural extent of healed Q-wave and non-Q-wave myocardial infarction. *Lancet* 2001; 357:21–28. [\[CrossRef\]](#)
19. Mahrholdt H, Wagner A, Holly TA, et al. Reproducibility of chronic infarct size measurement by contrast-enhanced magnetic resonance imaging. *Circulation* 2002; 106:2322–2327. [\[CrossRef\]](#)
20. Dall'Armellina E, Karia N, Lindsay AC, et al. Dynamic changes of edema and late gadolinium enhancement after acute myocardial infarction and their relationship to functional recovery and salvage index. *Circ Cardiovasc Imaging* 2011; 4:228–236. [\[CrossRef\]](#)
21. Engblom H, Hedström E, Heiberg E, Wagner GS, Pahlm O, Arheden H. Rapid initial reduction of hyperenhanced myocardium after reperfused first myocardial infarction suggests recovery of the periinfarction zone: one year follow up by MRI. *Circ cardiovasc imaging* 2009; 2:47–55.
22. Ibrahim T, Makowski MR, Jankauskas A, et al. Serial contrast-enhanced cardiac magnetic resonance imaging demonstrates regression of hyperenhancement within the coronary artery wall in patients after acute myocardial infarction. *JACC Cardiovasc imaging* 2009; 2:580–588.
23. McNamara MT, Higgins CB. Magnetic resonance imaging of chronic myocardial infarcts in man. *AJR Am J Roentgenol* 1986; 146:315–320. [\[CrossRef\]](#)
24. Higgins DM, Ridgway JP, Radjenovic A, Sivananthan UM, Smith MA. T1 measurement using a short acquisition period for quantitative cardiac applications. *Med Phys* 2005; 32:1738–1746. [\[CrossRef\]](#)
25. Messroghli DR, Radjenovic A, Kozerke S, Higgins DM, Sivananthan MU, Ridgway JP. Modified look-locker inversion recovery (MOLLI) for high-resolution T1 mapping of the heart. *Magn Reson Med* 2004; 52:141–146. [\[CrossRef\]](#)
26. Messroghli DR, Plein S, Higgins DM, et al. Human myocardium: single-breath-hold MR T1 mapping with high spatial resolution—reproducibility study. *Radiology* 2006; 238:1004–1012.
27. Bottomley PA, Foster TH, Argersinger RE, Pfeifer LM. A review of normal tissue hydrogen NMR relaxation times and relaxation mechanisms from 1–100 MHz: dependence on tissue type, NMR frequency, temperature, species, excision, and age. *Med Phys* 1984; 11:425–448. [\[CrossRef\]](#)
28. Rudolph A, Abdel-Aty H, Bohl S, et al. Noninvasive detection of fibrosis applying contrastenhanced cardiac magnetic resonance in different forms of left ventricular hypertrophy relation to remodeling. *J Am Coll Cardiol* 2009; 53:284–291. [\[CrossRef\]](#)